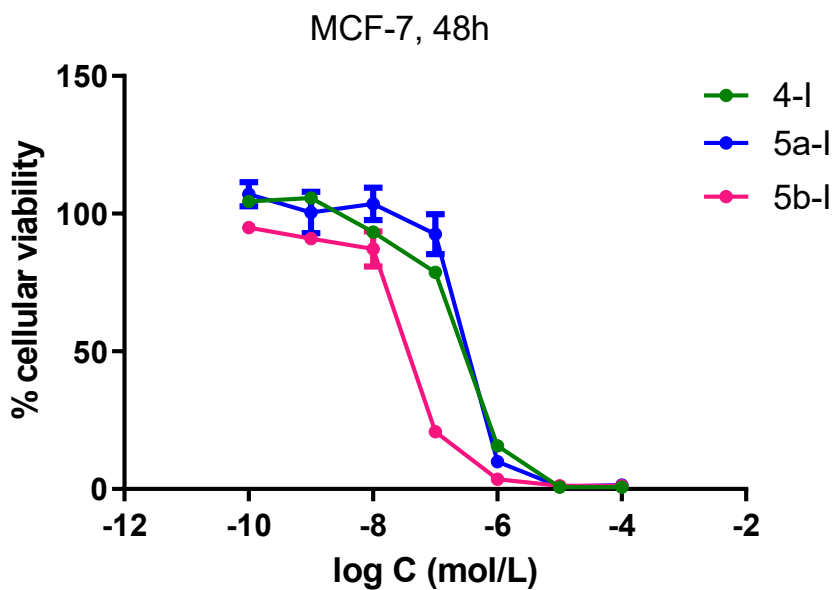
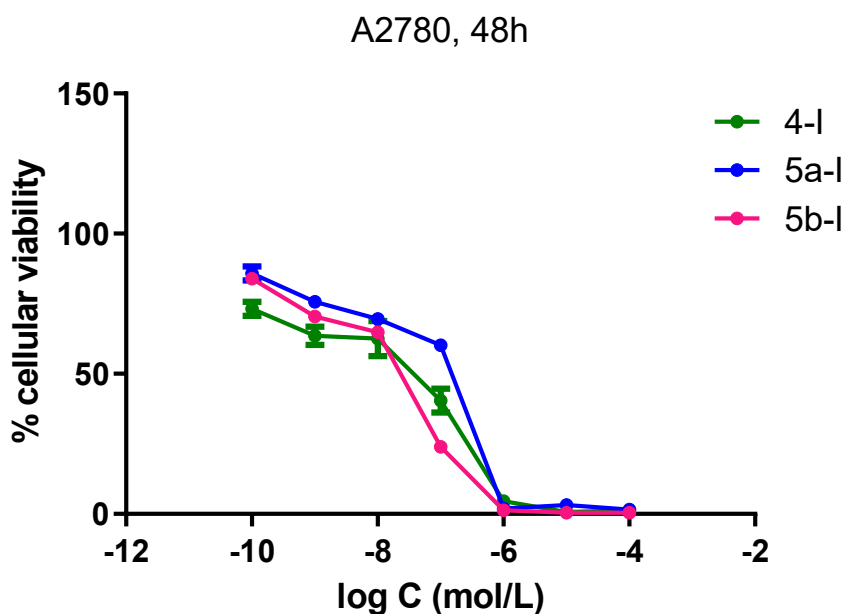


## Supporting Information

### Exploiting Click-Chemistry: Backbone Post-functionalisation of Homoleptic Gold(I) 1,2,3-triazole-5-ylidene Complexes

Leon F. Richter, Fernanda Marques, João D. G. Correia, Alexander Pöthig and Fritz E. Kühn



# Analytical Data

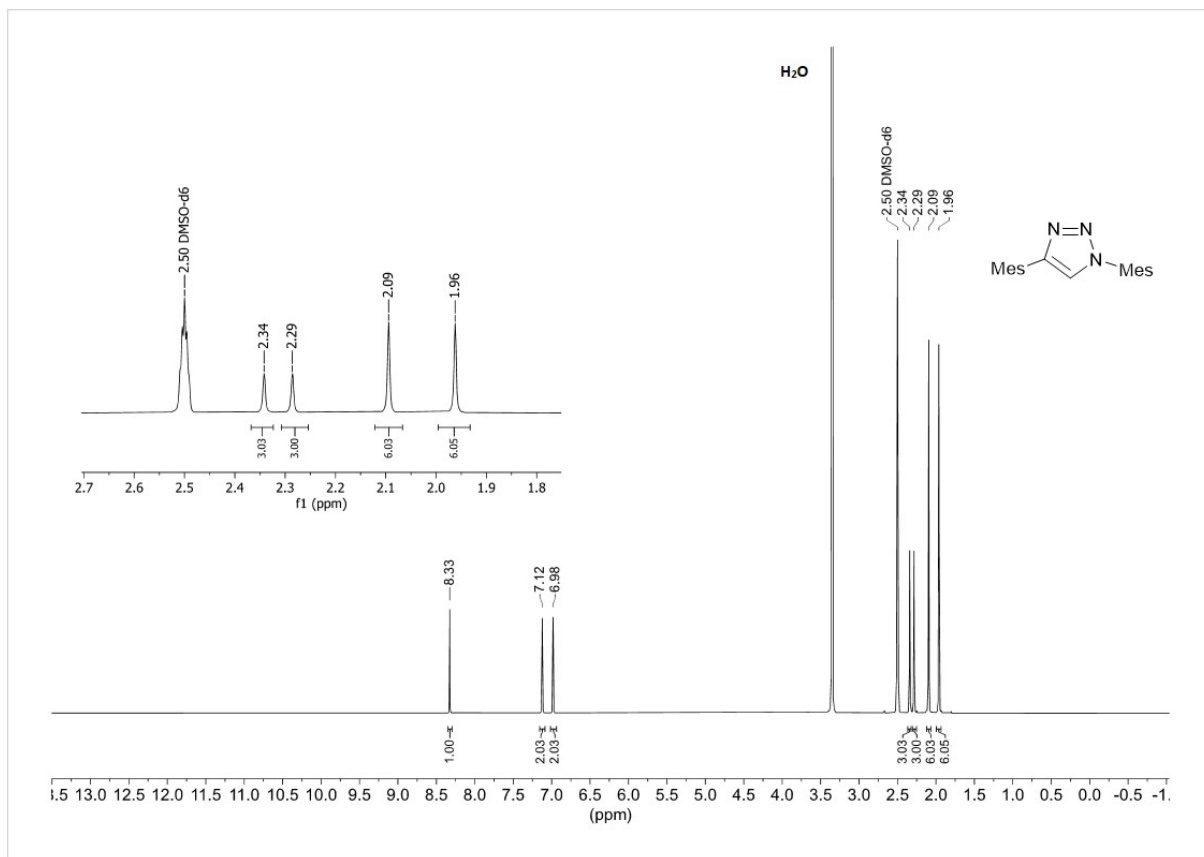


Figure 1:  $^1\text{H-NMR}$  spectrum of **1** in  $\text{DMSO-}d_6$ .

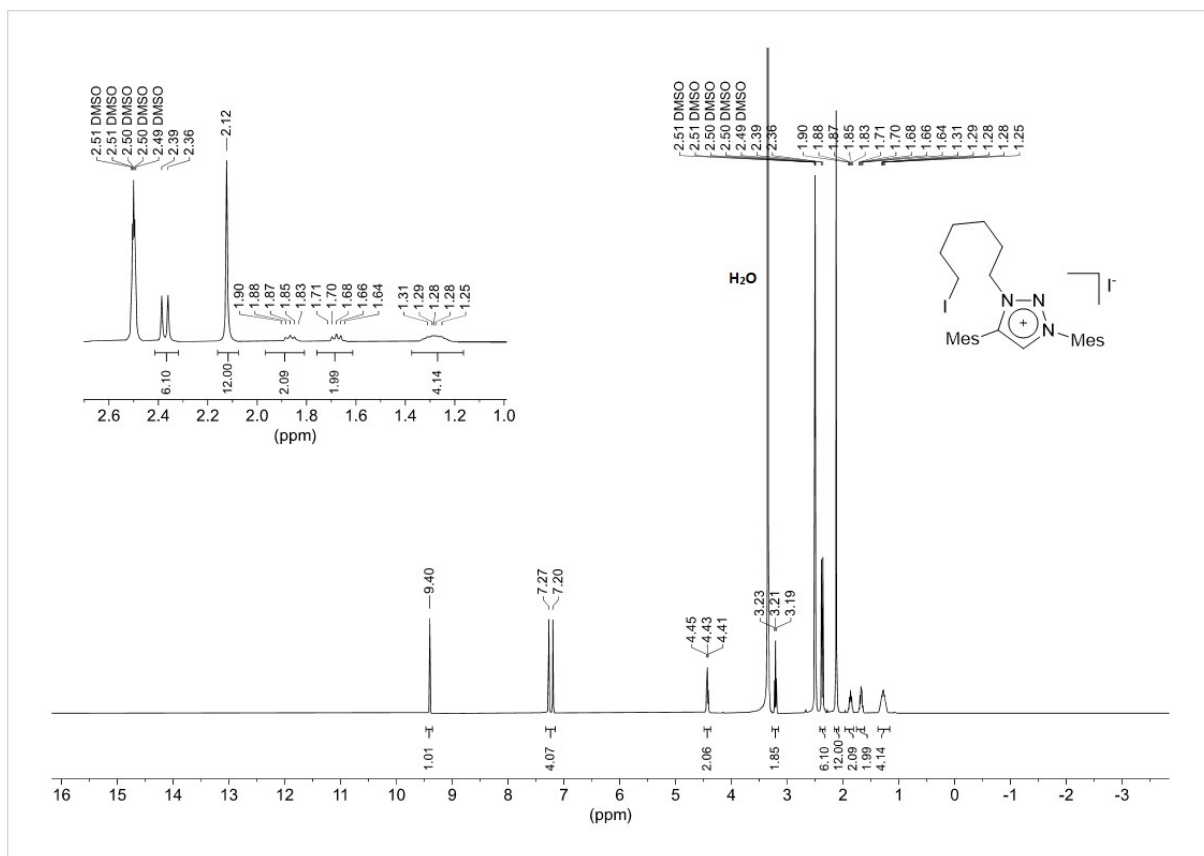


Figure 2:  $^1\text{H-NMR}$  spectrum of **2** in  $\text{DMSO-}d_6$ .

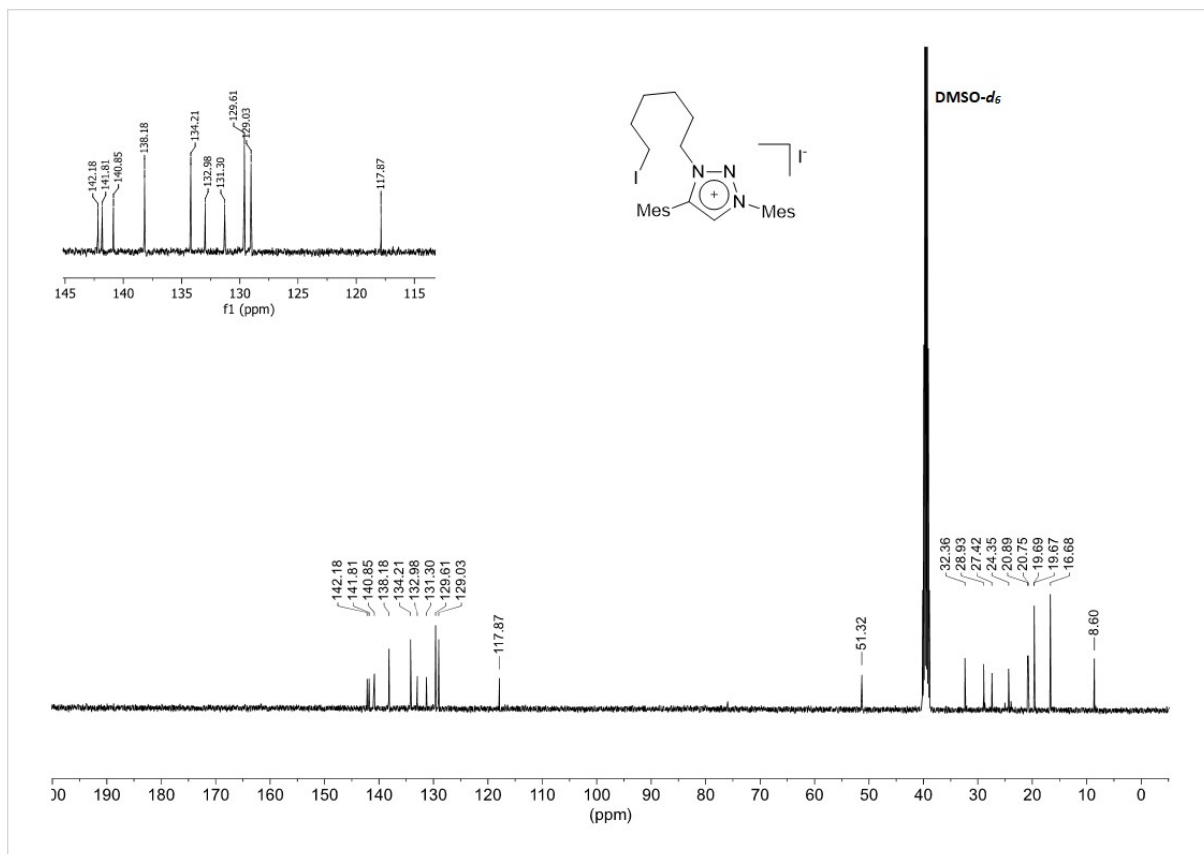


Figure 3:  $^{13}\text{C-NMR}$  spectrum of **2** in  $\text{DMSO-}d_6$ .

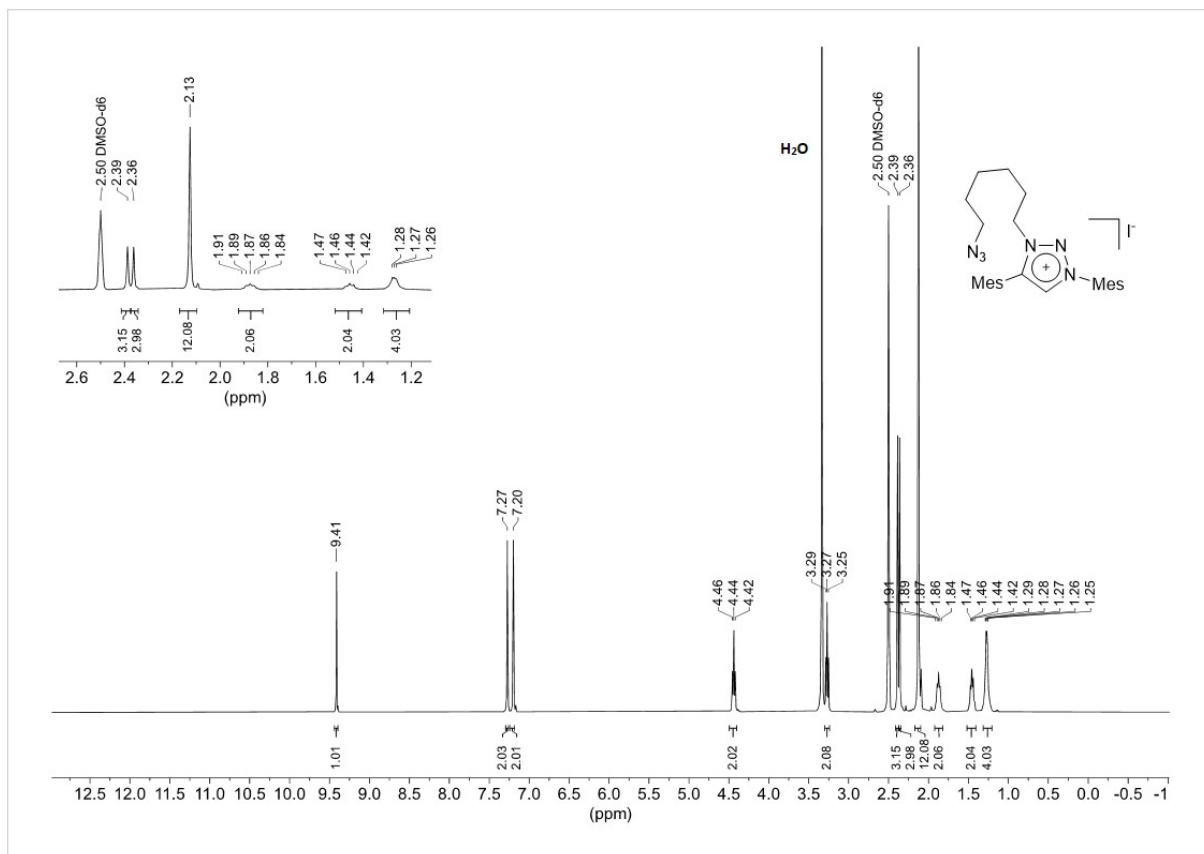


Figure 4:  $^1\text{H-NMR}$  spectrum of **3** in  $\text{DMSO-}d_6$ .

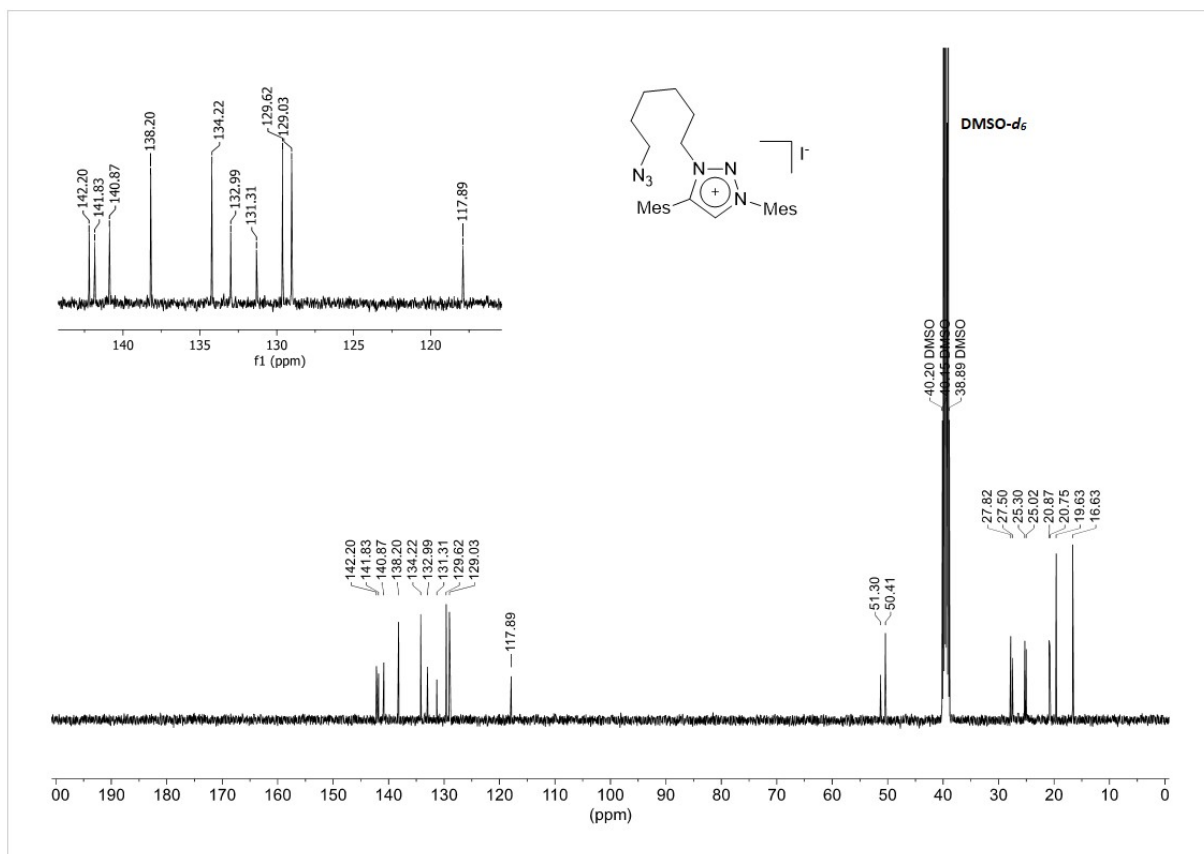


Figure 5:  $^{13}\text{C-NMR}$  spectrum of **3** in  $\text{DMSO-}d_6$ .

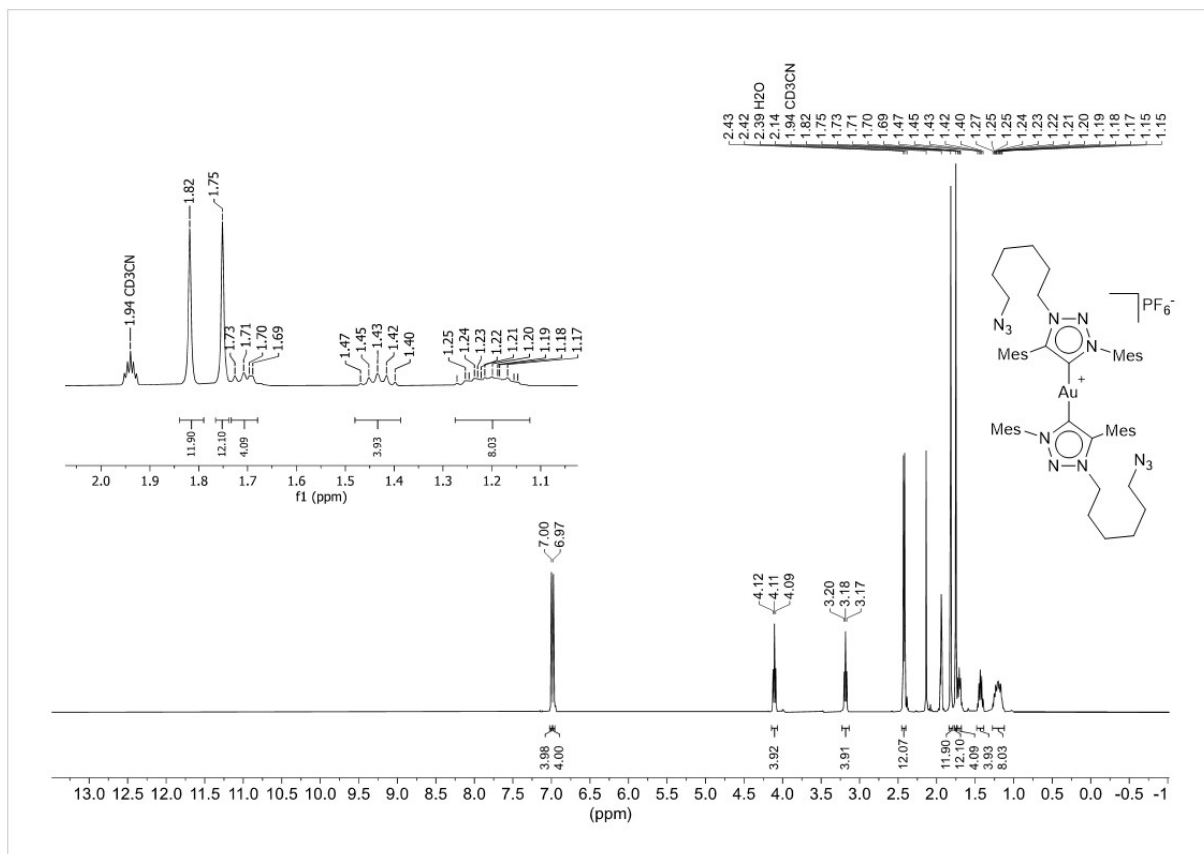


Figure 6: <sup>1</sup>H-NMR spectrum of **4** in CD<sub>3</sub>CN.

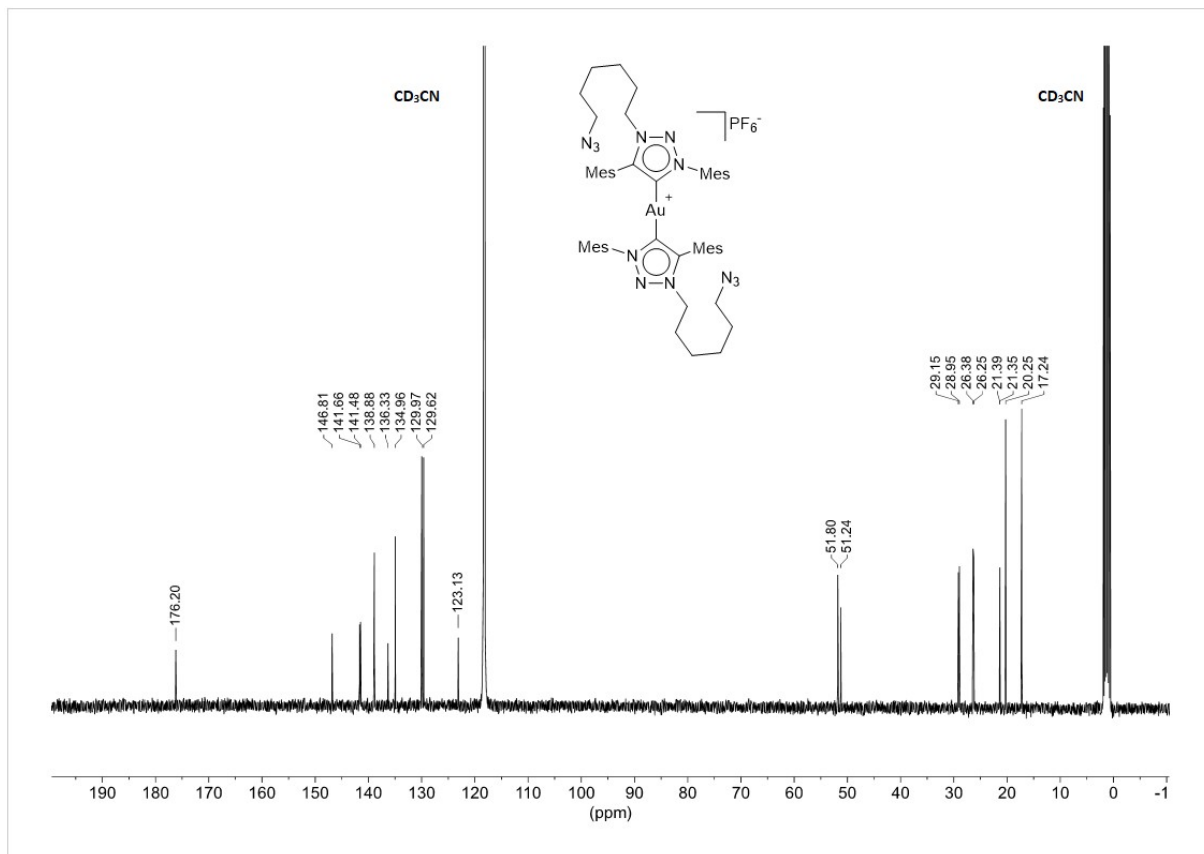


Figure 7: <sup>13</sup>C-NMR spectrum of **4** in CD<sub>3</sub>CN.

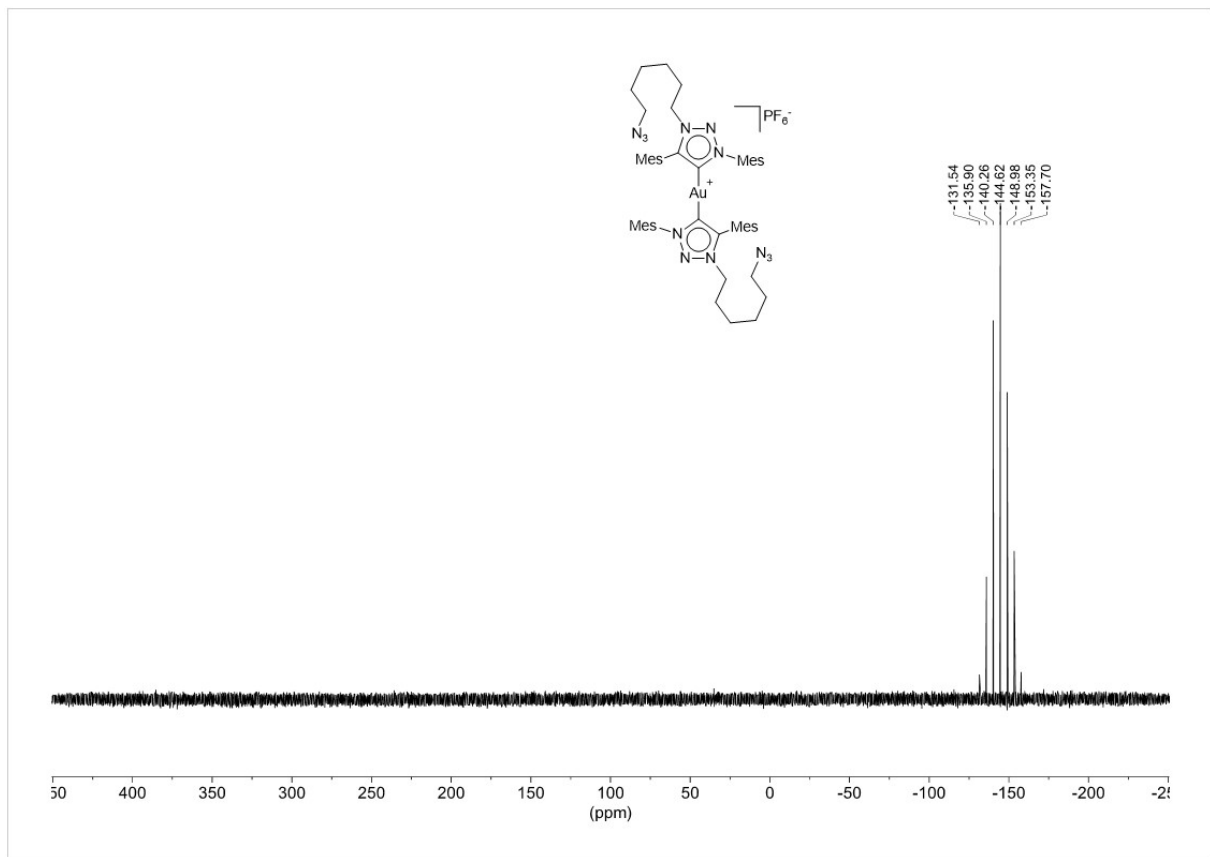


Figure 8: <sup>31</sup>P-NMR spectrum of **4**-PF<sub>6</sub> in CD<sub>3</sub>CN.

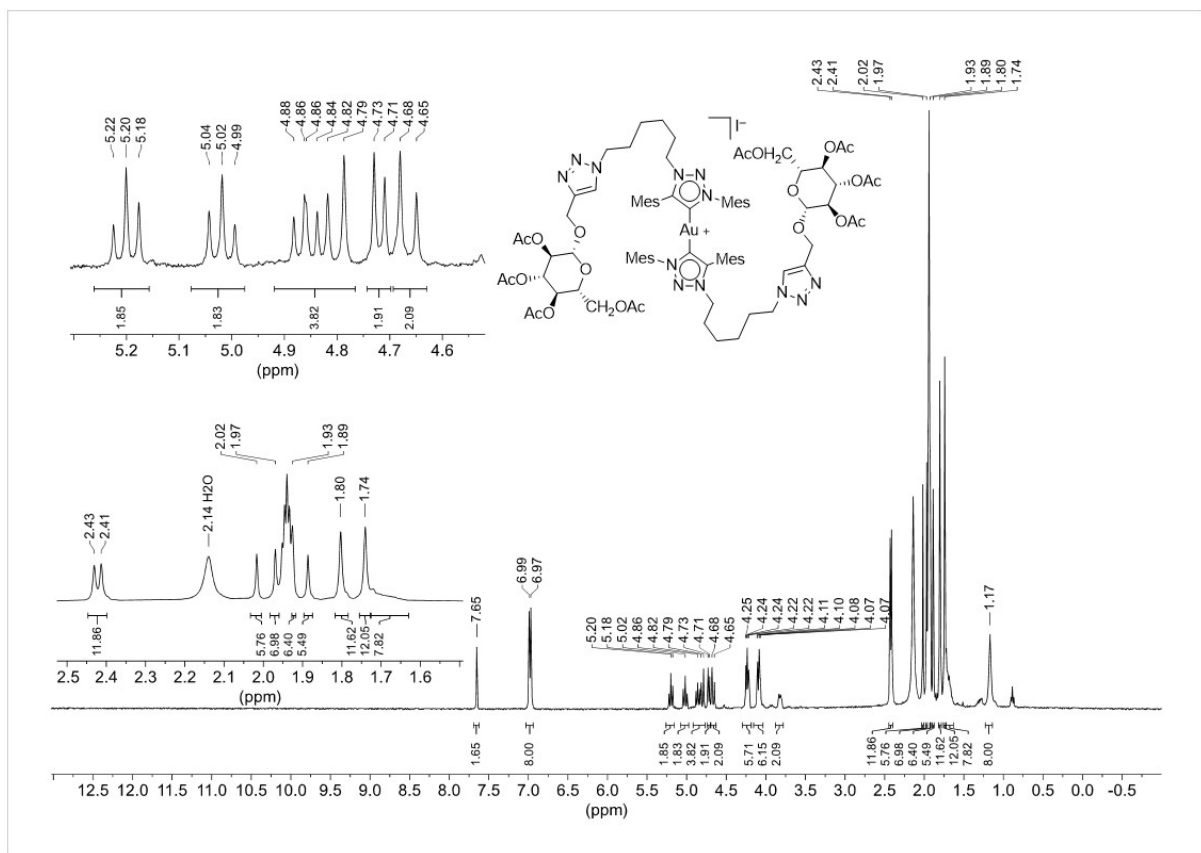


Figure 9: <sup>1</sup>H-NMR spectrum of **5a-I** in CD<sub>3</sub>CN.

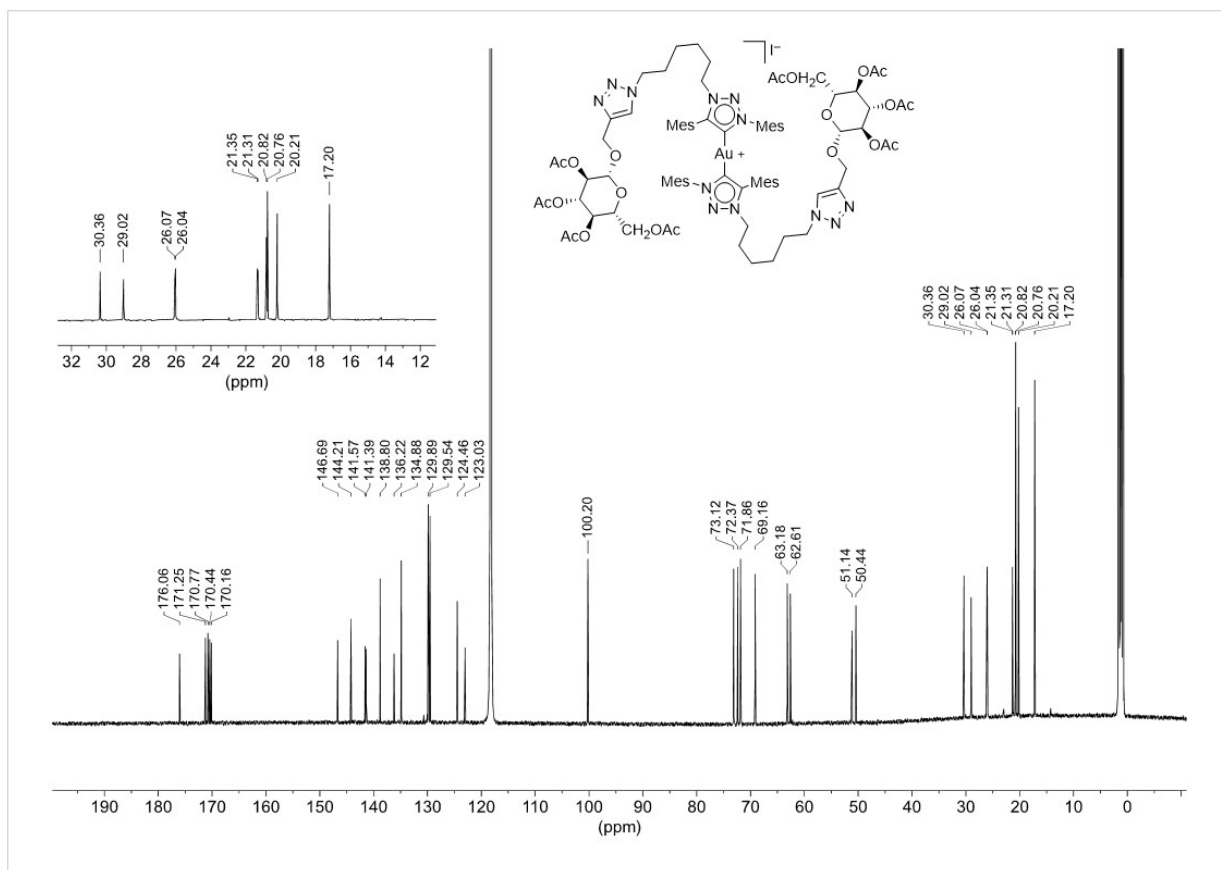


Figure 10:  $^{13}\text{C}$ -NMR spectrum of **5a-I** in  $\text{CD}_3\text{CN}$ .

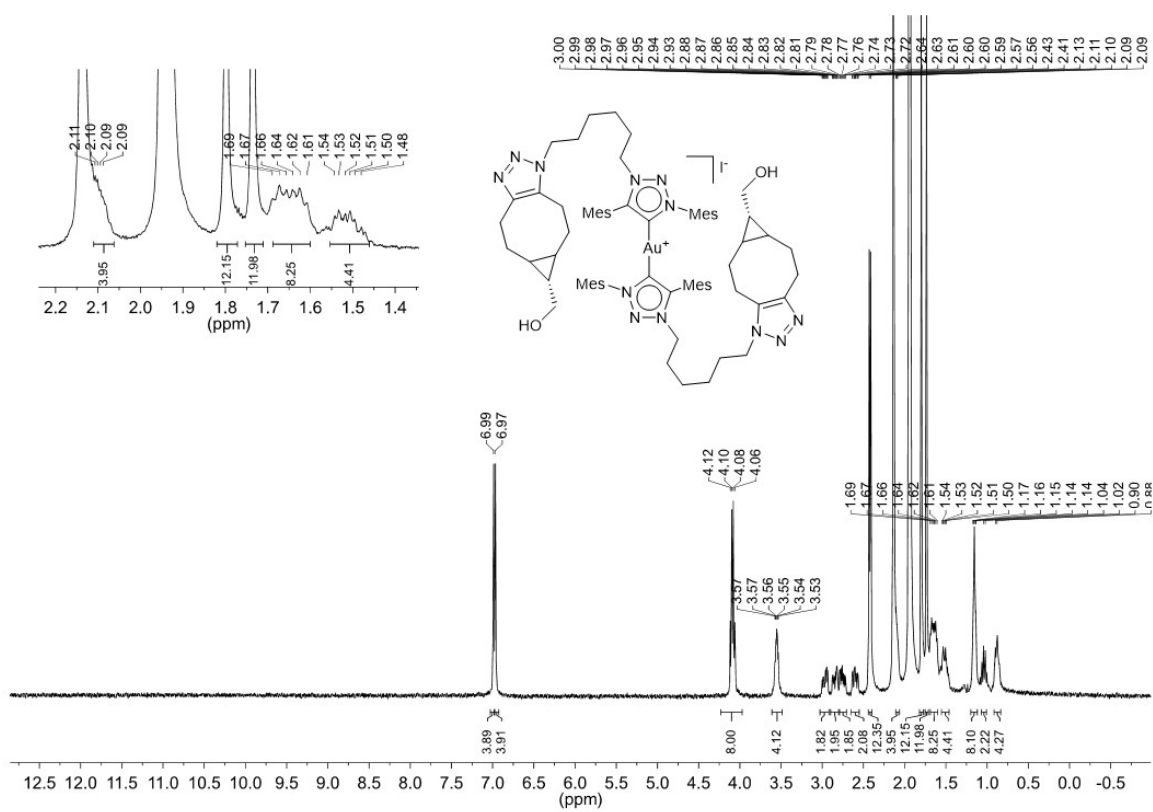


Figure 11:  $^1\text{H}$ -NMR spectrum of **5b-I** in  $\text{CD}_3\text{CN}$ .

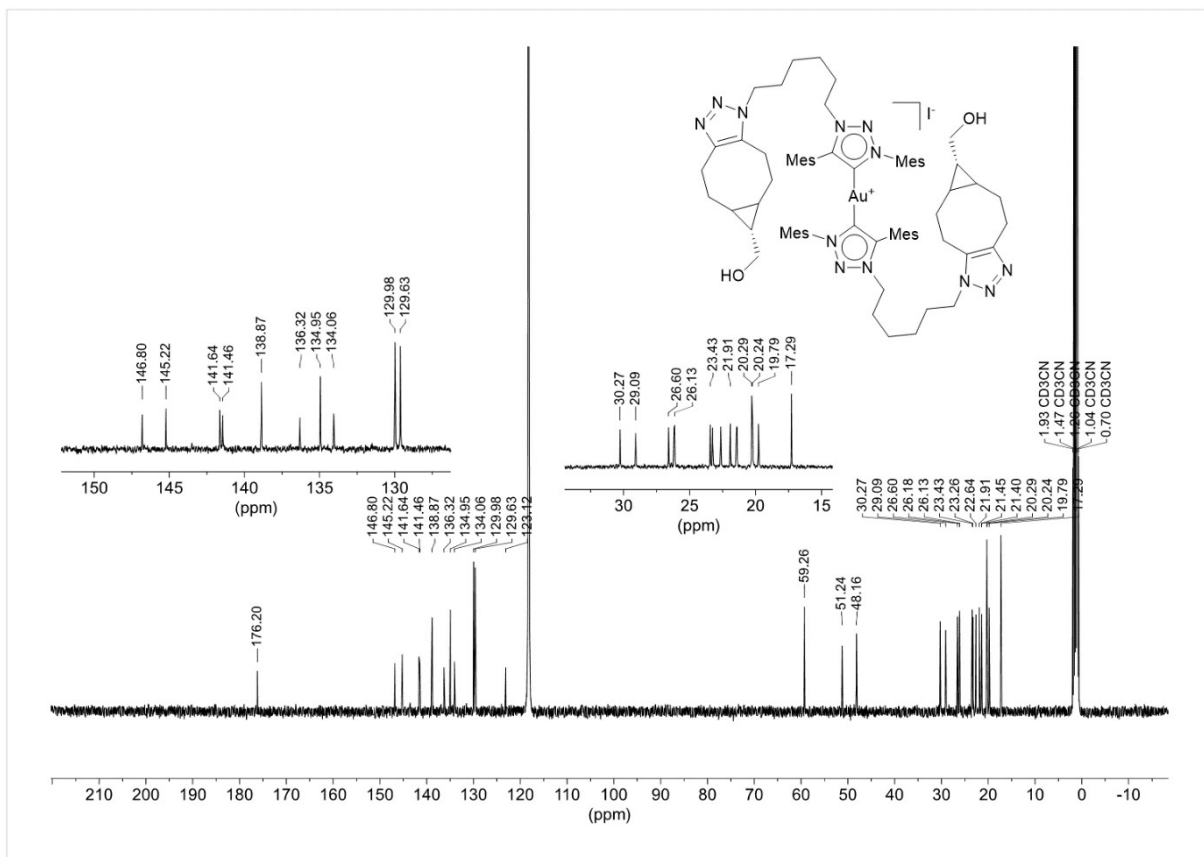


Figure 12:  $^{13}\text{C}$ -NMR spectrum of **5b-I** in  $\text{CD}_3\text{CN}$ .

Ir80027 #17-56 RT: 0.21-0.56 AV: 40 NL: 1.76E5  
T: ITMS + c ESI Full ms [50.00-1000.00]

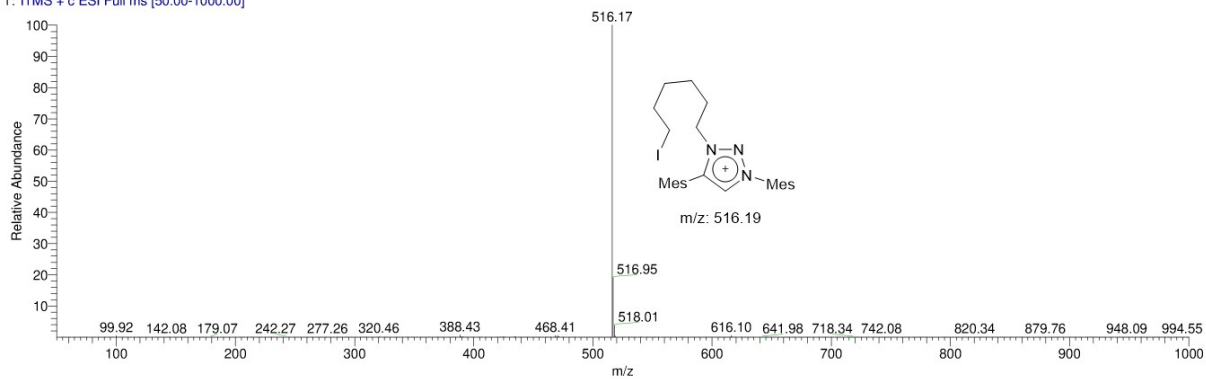


Figure 13: ESI-MS spectrum of **2**.

Ir87117 #11-22 RT: 0.13-0.23 AV: 12 NL: 8.09E4  
T: ITMS + c ESI Full ms [50.00-1000.00]

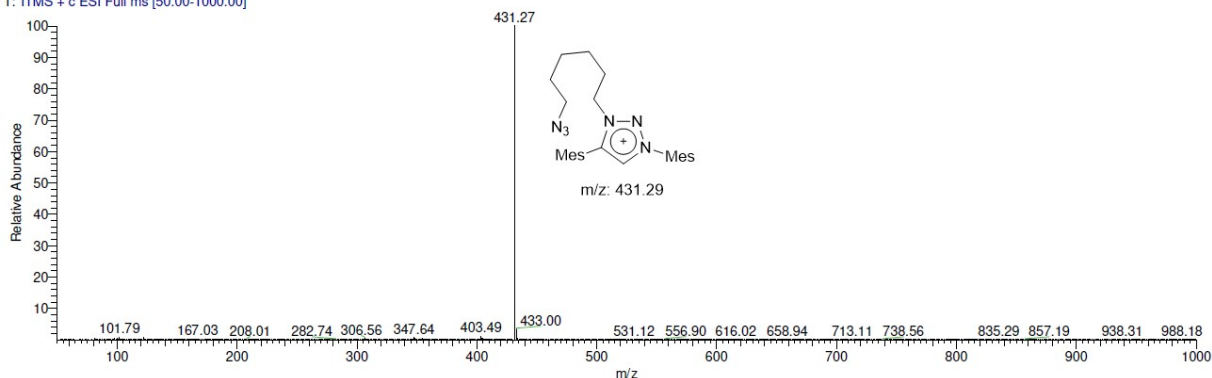


Figure 14: ESI-MS spectrum of **3**.



Ir85561 #29-50 RT: 0.47-0.78 AV: 22 NL: 2.83E4  
T: ITMS + c ESI Full ms [100.00-2000.00]

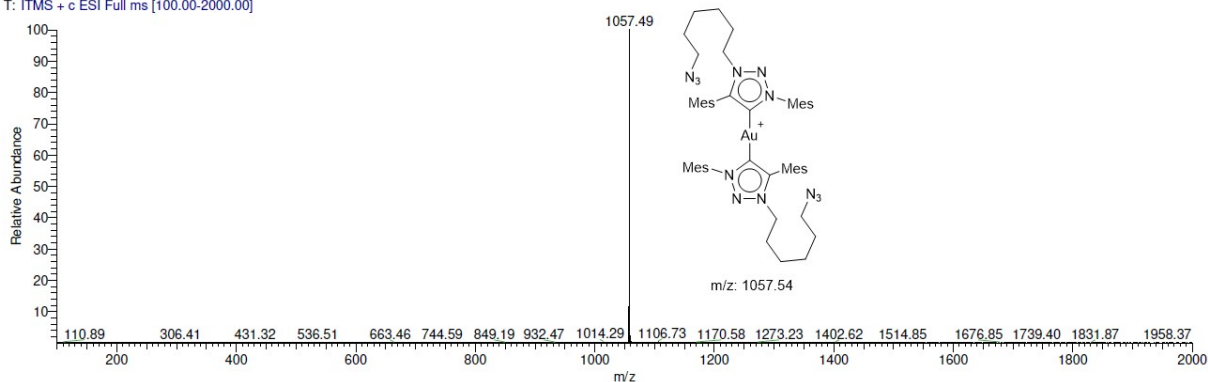


Figure 15: ESI-MS spectrum of 4-I.

Ir86176 #10-21 RT: 0.15-0.29 AV: 12 NL: 1.92E4  
T: ITMS + c ESI Full ms [100.00-2000.00]

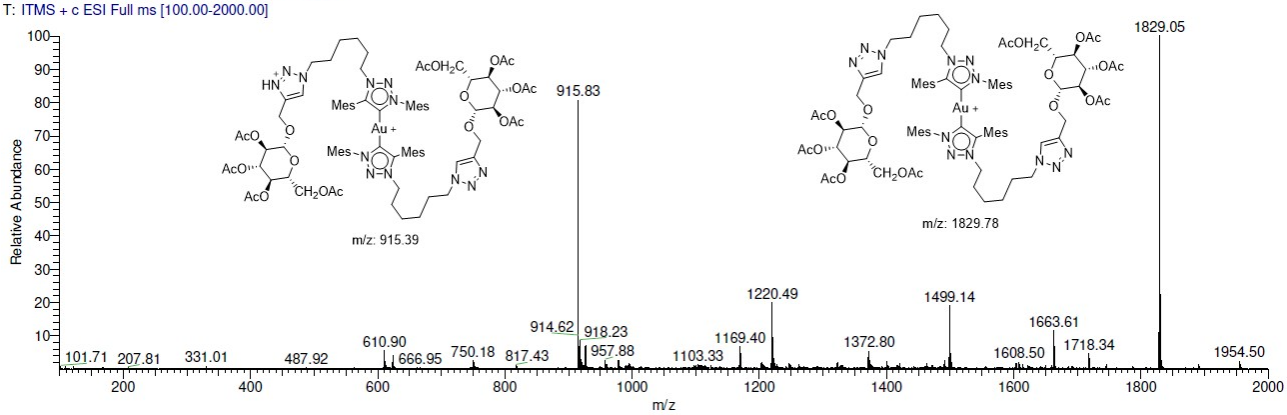


Figure 16: ESI-MS spectrum of 5a-I.

Ir86175 #8-22 RT: 0.12-0.30 AV: 15 NL: 9.72E4  
T: ITMS + c ESI Full ms [100.00-2000.00]

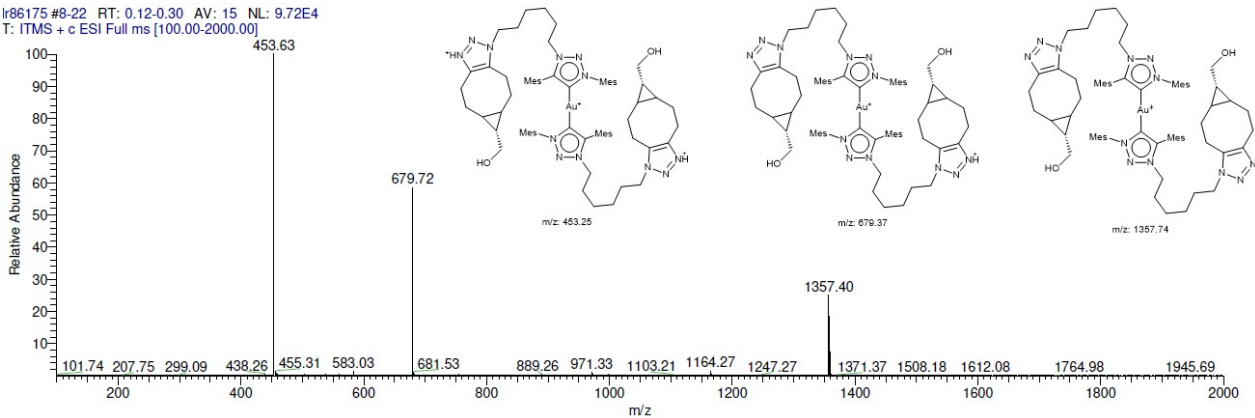


Figure 17: ESI-MS spectrum of 5b-I.

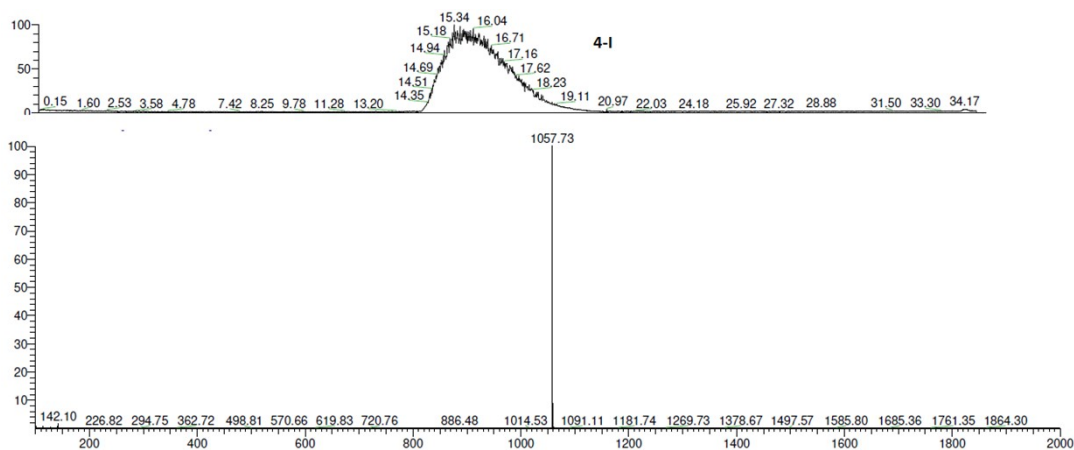


Figure 18 Analytical RP-HPLC of 4-I (85-100% MeCN/H<sub>2</sub>O with 0.1% formic acid, 25 min).

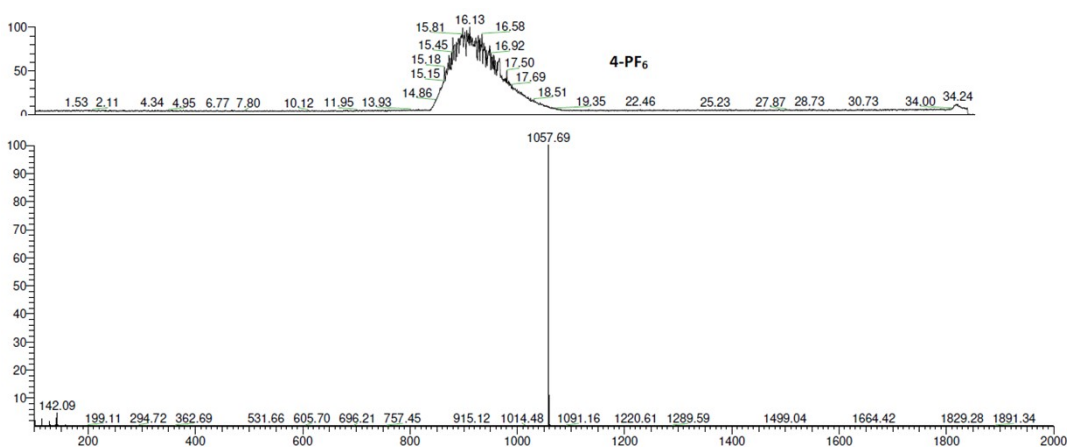


Figure 19 Analytical RP-HPLC of 4-PF<sub>6</sub> (85-100% MeCN/H<sub>2</sub>O with 0.1% formic acid, 25 min).

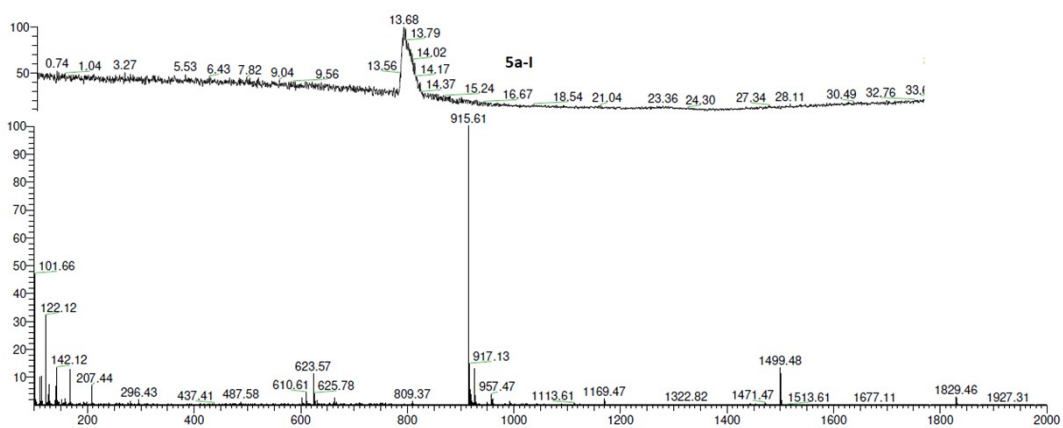


Figure 20 Analytical RP-HPLC of 5a-I (50-100% MeCN/H<sub>2</sub>O with 0.1% formic acid, 25 min).

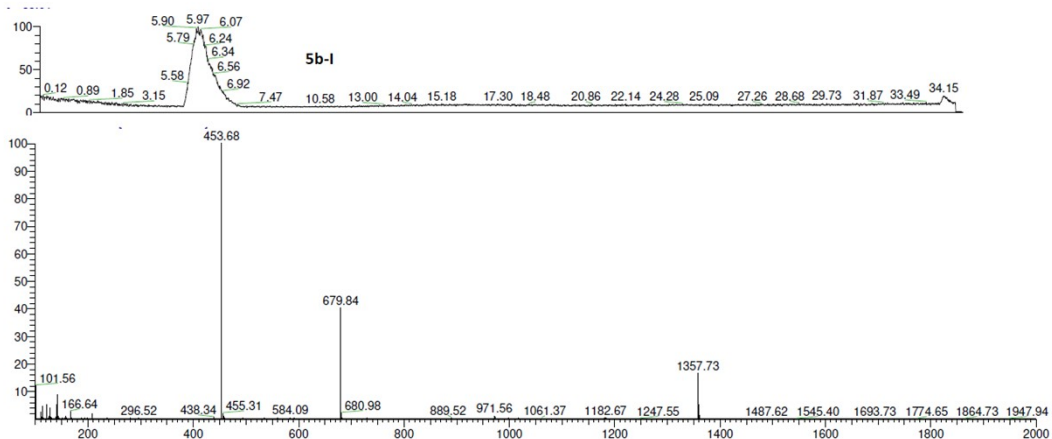


Figure 21 Analytical RP-HPLC of **5b-I** (85-100% MeCN/H<sub>2</sub>O with 0.1% formic acid, 25 min).

Table 1: Crystallographic data of compound 4-I; CCDC: 2268759.

<b>Chemical formula</b>	<b>C<sub>52</sub>H<sub>68</sub>AuIN<sub>12</sub></b>	
<b>Formula weight</b>	1185.06	
<b>Wavelength</b>	0.71073 Å	
<b>Crystal size</b>	0.021 x 0.136 x 0.154 mm	
<b>Crystal system</b>	triclinic	
<b>Space group</b>	<i>P</i> - 1	
<b>Unit cell dimensions</b>	<i>a</i> = 11.6459(8) Å	<i>α</i> = 106.185(2)°
	<i>b</i> = 15.3742(9) Å	<i>β</i> = 100.478(2)°
	<i>c</i> = 15.6241(9) Å	<i>γ</i> = 91.602(2)°
<b>Volume</b>	2632.6(3) Å <sup>3</sup>	
<b>Z</b>	2	
<b>Density (calculated)</b>	1.495 g/cm <sup>3</sup>	
<b>Absorption coefficient</b>	3.427 mm <sup>-1</sup>	
<b>F(000)</b>	1192	

Table 2: Data Collection and Structure Refinement of Compound 4-I

<b>Diffractometer</b>	Bruker Photon II
<b>Radiation source</b>	μS microfocus source (Mo)

<b>Theta range for data collection</b>	2.03 to 25.68°	
<b>Index ranges</b>	-14≤h≤14, -18≤k≤18, -19≤l≤19	
<b>Reflections collected</b>	57455	
<b>Independent reflections</b>	9993 [R(int) = 0.0292]	
<b>Coverage of independent reflections</b>	99.9%	
<b>Absorption correction</b>	Multi-Scan	
<b>Max. and min. transmission</b>	0.7457 and 0.6177	
<b>Structure solution technique</b>	direct methods	
<b>Structure solution program</b>	SHELXT (Sheldrick, 2015)	
<b>Refinement method</b>	Full-matrix least-squares on F <sup>2</sup>	
<b>Refinement program</b>	SHELXL (Sheldrick, 2017), SHELXLE (Huebschle, 2011)	
<b>Function minimized</b>	$\sum w(F_o^2 - F_c^2)^2$	
<b>Data / restraints / parameters</b>	9993 / 0 / 607	
<b>Goodness-of-fit on F2</b>	1.140	
<b><math>\Delta/\sigma_{\max}</math></b>	0.003	
<b>Final R indices</b>	9538 data; $l > 2\sigma(l)$	$R_1 = 0.0256, wR_2 = 0.0546$
	all data	$R_1 = 0.0276, wR_2 = 0.0553$
<b>Weighting scheme</b>	$w=1/[\Sigma^2(F_o^2)+(0.0108P)^2+6.5216P]$ where $P=(F_o^2+2F_c^2)/3$	
<b>Largest diff. peak and hole</b>	1.665 and -1.032 eÅ <sup>-3</sup>	
<b>R.M.S. deviation from mean</b>	0.080 eÅ <sup>-3</sup>	

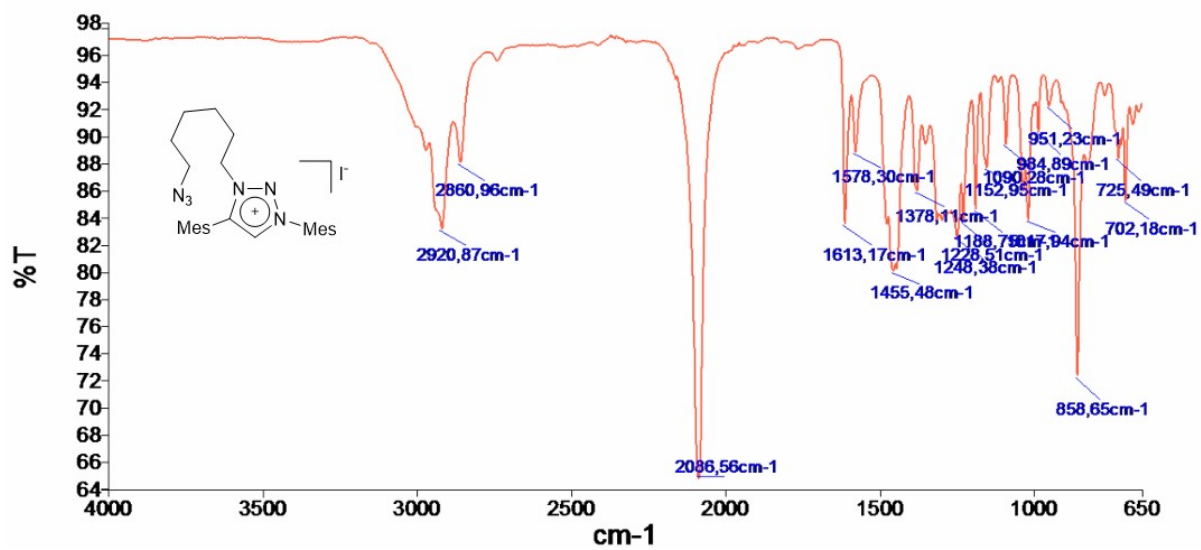


Figure 22: FT-IR spectrum of 3.

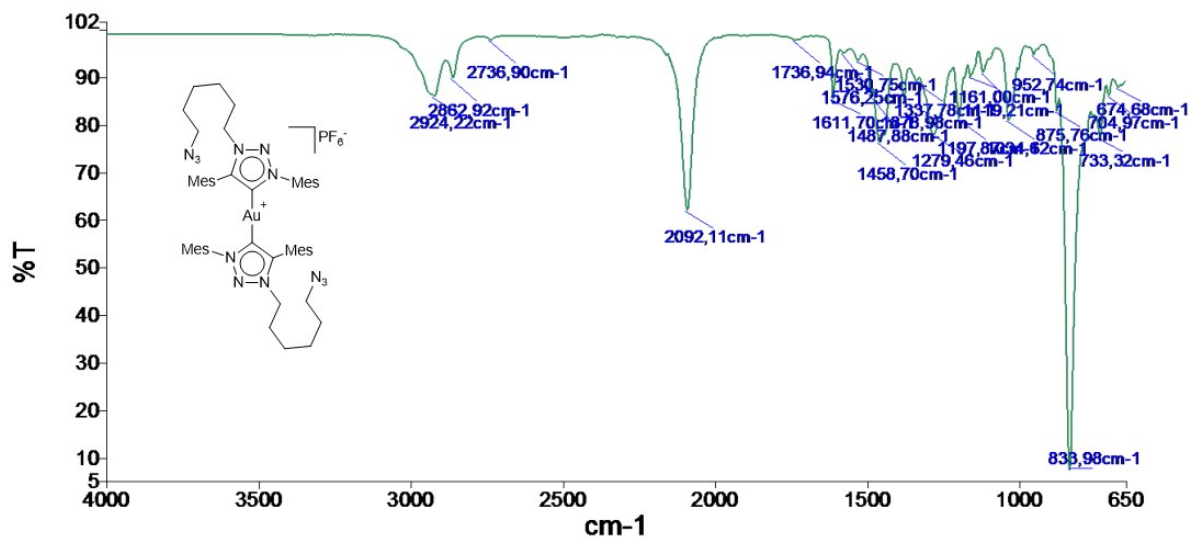


Figure 23: FT-IR spectrum of 4.

## References

- [1] Bruker AXS, **n.d.**
- [2] C. B. Hübschle, G. M. Sheldrick, B. Dittrich, *J. Appl. Crystallogr.* **2011**, *44*, 1281–1284.
- [3] G. M. Sheldrick, *Acta Crystallogr. Sect. C Struct. Chem.* **2015**, *71*, 3–8.
- [4] A. J. Wilson, *International Tables for Crystallography*, Kluwer Academic Publishers: Dordrecht, **1992**.
- [5] A. L. Spek, *Acta Crystallogr. Sect. D Biol. Crystallogr.* **2009**, *65*, 148–155.
- [6] F. L. Breusch, F. Baykut, *Chem. Ber.* **1953**, *86*, 684–688.
- [7] R. Uson, A. Laguna, M. Laguna, D. A. Briggs, H. H. Murray, J. P. Fackler Jr, *Inorg. Synth.* **1989**, *26*, 85–91.
- [8] K. Barral, A. D. Moorhouse, J. E. Moses, *Org. Lett.* **2007**, *9*, 1809–1811.